

# The intrinsic constraint approach to cue combination: An empirical and theoretical evaluation

**Kevin J. MacKenzie**

Centre for Vision Research and Department of Psychology,  
York University, Toronto, ON, Canada, &  
School of Psychology, Bangor University, Bangor, UK



**Richard F. Murray**

Centre for Vision Research and Department of Psychology,  
York University, Toronto, ON, Canada



**Laurie M. Wilcox**

Centre for Vision Research and Department of Psychology,  
York University, Toronto, ON, Canada



We elucidate two properties of the intrinsic constraint (IC) model of depth cue combination (F. Domini, C. Caudek, & H. Tassinari, 2006). First, we show that IC combines depth cues in a weighted sum that maximizes the signal-to-noise ratio of the combined estimate. Second, we show that IC predicts that any two depth-matched pairs of stimuli are separated by equal numbers of just noticeable differences (JNDs) in depth. That is, IC posits a strong link between perceived depth and depth discrimination, much like some Fechnerian theories of sensory scaling. We test this prediction, and we find that it does not hold. We also find that depth discrimination performance approximately follows Weber's law, whereas IC assumes that depth discrimination thresholds are independent of baseline stimulus depth.

Keywords: depth perception, cue combination, modified weak fusion, intrinsic constraint

Citation: MacKenzie, K. J., Murray, R. F., & Wilcox, L. M. (2008). The intrinsic constraint approach to cue combination: An empirical and theoretical evaluation. *Journal of Vision*, 8(8):5, 1–10, <http://journalofvision.org/8/8/5/>, doi:10.1167/8.8.5.

## Introduction

Many visual cues carry information about the depth of an object, and an active topic of research is how the human visual system combines two or more such cues to arrive at a single estimate of depth. Most studies of cue combination have used the framework of the modified weak fusion (MWF) model (Landy, Maloney, Johnston, & Young, 1995; Maloney & Landy, 1989), but recently Domini, Caudek, and Tassinari (2006) have proposed an alternative account of depth cue combination, which they call the intrinsic constraint (IC) model. In this article, we derive two properties of the IC model and test one of them experimentally. First, we show that IC effectively combines depth cues in an optimal weighted sum. Second, we show that IC predicts a strong link between perceived depth and depth discrimination, and we report a psychophysical experiment that does not support this prediction.

## Cue combination models

MWF, the most widely used model of cue combination, assumes that the visual system has access to two or more depth cues that give metric depth estimates in a common unit of measurement. These cues are assumed to be

degraded by statistically independent Gaussian noise. The cues are represented as random variables, say  $B(z)$  for depth from binocular disparity and  $M(z)$  for depth from structure-from-motion, where  $z$  is the true depth of the point of interest. MWF posits that the visual system combines these cues in a weighted sum:  $C(z) = w_B B(z) + w_M M(z)$ . The weights  $w_B$  and  $w_M$  are non-negative and sum to one, but otherwise they are arbitrary constants. However, if the weights are set to  $w_B = \sigma_B^{-2} / (\sigma_B^{-2} + \sigma_M^{-2})$  and  $w_M = \sigma_M^{-2} / (\sigma_B^{-2} + \sigma_M^{-2})$ , where  $\sigma_B = SD[B(z)]$  and  $\sigma_M = SD[M(z)]$ , then the sum is optimal in the sense that it maximizes the signal-to-noise ratio (SNR) of the combined estimate  $C(z)$ , defined as  $SNR[C(z)] = E[C(z)] / SD[C(z)]$ . Here,  $E$  denotes expected value and  $SD$  denotes standard deviation (for an extensive review, see Landy et al., 1995).

In this very brief summary, we have highlighted the aspects of MWF that are most relevant to our discussion of IC. Important parts of MWF that we will not discuss at length include a *promotion* stage, in which direct retinal measurements of depth cues like disparity and motion are scaled to give metric depth estimates (possibly biased or unbiased, but always in a physically meaningful, metric unit of depth); extensions to accommodate correlated noise across cues (Oruç, Maloney, & Landy, 2003); and a *robustness* mechanism in which a depth cue that is discrepant with other depth cues can be weighted less heavily at the combination stage or even discarded.

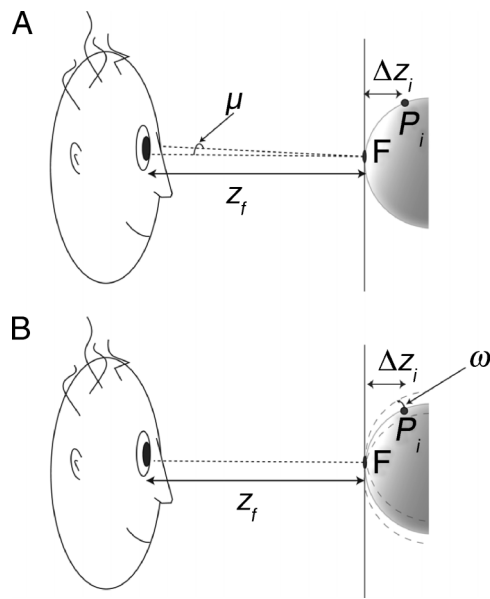


Figure 1. Small-angle approximations to depth cues. (A) Disparity. The observer has vergence angle  $\mu$  when fixating point F at distance  $z_f$ . The depth of the point of interest  $P_i$  is  $z_f + \Delta z_i$ . Domini et al. (2006) show that  $P_i$  has absolute retinal disparity approximately equal to  $\mu \Delta z_i / z_f$ . (B) Retinal velocity. The object rotates about a horizontal axis through the fixation point F, and  $P_i$  moves through a small angle  $\omega$  in a short time  $\Delta t$ . Domini et al. show that  $P_i$  has retinal velocity approximately equal to  $\omega \Delta z_i / z_f$ .

MWF has received extensive experimental support since it was proposed by Maloney and Landy (1989) and extended in later work (Johnston, Cumming, & Landy, 1994; Landy et al., 1995; Young, Landy, & Maloney, 1993), and many studies have demonstrated that cues to depth are combined optimally (e.g., Ernst & Banks, 2002; Hillis, Watt, Landy, & Banks, 2004; Jacobs, 1999). A further strength of MWF is its simplicity: Given multiple independent depth cues, taking a weighted average is a reasonable and easily understood strategy for combining them.

The IC model has recently been proposed as an alternative account of depth cue combination. This model assumes that the visual system has access to depth cues from binocular disparity and retinal motion, but only that these cues are *proportional* to true depth. To support this assumption, Domini et al. (2006) show that in a small-angle approximation, both absolute binocular disparity and retinal velocity of a point on a rotating object are proportional to true depth (see Figure 1). IC represents these depth cues as random variables: disparity  $D(z) = \mu z + \epsilon_D$  and retinal velocity  $V(z) = \omega z + \epsilon_V$ , where  $\mu$  is the observer’s vergence angle,  $\omega$  is the angle through which the object rotates in a small time interval  $\Delta t$ ,  $z$  is the point of interest’s true depth, and  $\epsilon_D$  and  $\epsilon_V$  are independent zero-mean, Gaussian noise sources with fixed standard deviations  $\sigma_D$  and  $\sigma_V$ , respectively. The depth variable  $z$  refers to *scaled depth*, defined as the depth of the point

of interest relative to the fixation point, divided by the distance from the observer to the fixation point (see Figure 1).

IC assumes that we have simultaneous depth cue measurements at several different locations on an object. If the true depths at these locations are  $z_1, \dots, z_n$ , then the disparity measurements are independent samples from the random variables  $D(z_1), \dots, D(z_n)$ , and we will denote these samples by  $d_1, \dots, d_n$ . Similarly, the retinal velocity measurements are samples from  $V(z_1), \dots, V(z_n)$ , which we will denote by  $v_1, \dots, v_n$ . The goal of IC is to use these measurements to arrive at a single depth estimate for each object location. This occurs in several steps (see Figure 2).

1. Each depth cue measurement is divided by the standard deviation of the random variable it is drawn from to produce a normalized depth cue measurement:  $\bar{d}_i = d_i / \sigma_D$ ,  $\bar{v}_i = v_i / \sigma_V$ .
2. The normalized depth cue measurements are grouped into ordered pairs  $(\bar{d}_i, \bar{v}_i)$ , where each pair consists of the normalized disparity and velocity measurements at object location  $i$ . This gives a two-dimensional cloud of points.
3. The first principal component  $\vec{e}_1$  of this cloud of points is computed.
4. The dot product is taken between each ordered pair and the first principal component:  $\rho_i = (\bar{d}_i, \bar{v}_i) \cdot \vec{e}_1$ . IC postulates that depth discrimination is based on the decision variable  $\rho_i$ , and that perceived depth is some monotonically increasing function of  $\rho_i$ .

We will call the computation in steps 1–4 the *principal component projection* (PCP) algorithm. A later stage of

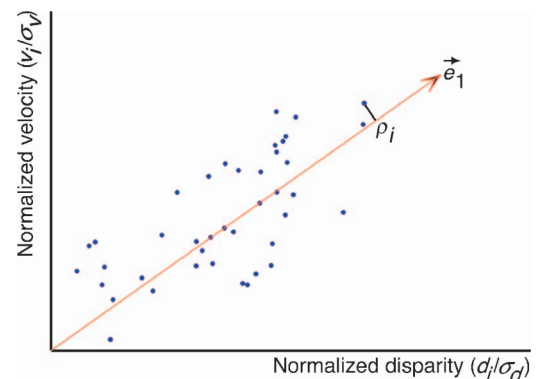


Figure 2. A schematic representation of the PCP algorithm. The x-component of each data point is a normalized disparity measurement from a point on the object being viewed, and the y-component is a normalized velocity measurement from the same point on the object. The unit-magnitude vector  $\vec{e}_1$  is the first principal component of the entire cloud of data points.  $\rho_i$  is the magnitude of the projection of a single data point onto  $\vec{e}_1$ . According to IC, the perceived depth of any point on the object is a monotonically increasing function of the value of  $\rho_i$  for that point.

IC, which we will not need to consider, determines the monotonic relationship between  $\rho_i$  and perceived depth.

One appeal of IC is that it uses quantities that can be measured directly from retinal images, namely absolute disparity and retinal velocity, with no need to scale the cues into a common, physically meaningful unit before cue combination, as in MWF. Furthermore, Domini et al. (2006) report experiments on perceived depth that are consistent with IC and inconsistent with MWF. They compare depth increment detection thresholds for stimuli defined by single or multiple cues (i.e., motion and/or disparity). Their results suggest that performance depends on whether the baseline stimulus is defined by single or multiple cues, a result that is not predicted by MWF.

## A reformulation

In this section, we show that IC's cue combination algorithm (PCP) effectively combines cues in an optimal weighted sum. The expected values of  $D(z) = \mu z + \varepsilon_D$  and  $V(z) = \omega z + \varepsilon_V$  are proportional<sup>1</sup> and so are the expected values of  $D(z)/\sigma_D$  and  $V(z)/\sigma_V$  from which the normalized depth cue measurements  $d_i$  and  $v_i$  are drawn:

$$E[V(z)/\sigma_V] = (\omega/\sigma_V)(\sigma_D/\mu)E[D(z)/\sigma_D]. \quad (1)$$

Thus, if the normalized depth cue measurements were noise-free, the scatterplot of ordered pairs  $(\bar{d}_i, \bar{v}_i)$  would lie on the line through the origin with slope  $(\omega/\sigma_V)(\sigma_D/\mu)$ , and its first principal component would be the vector  $(1, (\omega/\sigma_V)(\sigma_D/\mu))$  normalized to unit length:

$$\vec{e}_1 = \frac{(\mu/\sigma_D, \omega/\sigma_V)}{\left((\mu/\sigma_D)^2 + (\omega/\sigma_V)^2\right)^{1/2}}. \quad (2)$$

The standard deviation of both normalized depth cues is one, so the effect of the measurement noise is simply to displace the measurements  $(\bar{d}_i, \bar{v}_i)$  isotropically off this line, and in the limit of a large number of samples, the first principal component of this cloud of points is still given by Equation 2.

According to IC, perceived depth at object location  $i$  is a monotonic function of  $\rho_i$ :

$$\rho_i = (\bar{d}_i, \bar{v}_i) \vec{e}_1 \quad (3)$$

$$= (d_i/\sigma_D, v_i/\sigma_V) \frac{(\mu/\sigma_D, \omega/\sigma_V)}{\left((\mu/\sigma_D)^2 + (\omega/\sigma_V)^2\right)^{1/2}} \quad (4)$$

$$= \frac{(\mu/\sigma_D^2)d_i + (\omega/\sigma_V^2)v_i}{\left((\mu/\sigma_D)^2 + (\omega/\sigma_V)^2\right)^{1/2}}. \quad (5)$$

In Appendix A, we show how to combine two cues with different means and standard deviations in order to maximize the SNR of the resulting decision variable. Comparing Equations 5 and A5 shows that  $\rho_i$  is simply the optimal weighted sum of the disparity and the velocity cues, scaled to unit variance.

Domini et al. (2006) explain that the goal of their cue combination algorithm is “to obtain the best possible estimate of the affine structure of the distal depth” (p. 1709), and they show that IC sometimes makes the same psychophysical predictions as MWF (p. 1714), so we do not claim to have derived an entirely unexpected property of IC. To support their claim to have found an optimal combination method, though, Domini et al. only report a numerical simulation showing that PCP works best when the measurements  $d_i$  and  $v_i$  are normalized by  $\sigma_D$  and  $\sigma_V$ . From this simulation, it is unclear whether PCP is optimal in any broader sense, so we believe our derivation helps to clarify exactly what PCP accomplishes. Furthermore, we hope that highlighting IC's similarity to MWF will make it easier to relate IC to the existing cue combination literature.

Although both IC and MWF compute an optimal weighted sum, they can make different predictions about human performance because they assume different types of depth cues. Consider a structure-from-motion stimulus that has zero disparity because it is shown on a computer monitor. IC's PCP algorithm recognizes that the disparity cue does not covary with the motion cue and hence seems to convey no depth information, so IC effectively assigns zero weight to the disparity cue.<sup>2</sup> MWF assumes that all cues are valid depth estimates and so combines disparity and motion cues with weights determined by the cues' variances (unless a robustness mechanism rejects the disparity cue as being discrepant with other depth cues). Thus, both models compute optimal weighted sums, but they may weight cues differently because different notions of optimality follow from different assumptions about individual depth cues. Similarly, as mentioned above, Domini et al. (2006) also describe tasks where MWF and IC make different predictions.

We reiterate that Equation 2 for the first principal component is only asymptotically valid, in the limit of having depth cue measurements from a large number of object locations. Given few measurements, PCP will not give an exactly optimal weighted sum of individual cues. Thus, experiments that examine what weights are assigned to disparity and motion in impoverished stimuli like very sparse random-dot patterns might be able to test whether the visual system uses an algorithm like PCP to calculate optimal weighted sums.

## A JND-counting theory of perceived depth

MWF assumes that disparity and motion cues give properly scaled estimates of true depth, and this property is

preserved in the combined depth estimate by the requirement that the cue weights sum to one. IC assumes only that depth cues are proportional to true depth, generally with different constants of proportionality. Accordingly, IC is faced with the additional problem of scaling the cues to recover true depth. The first step in IC's solution to this problem is to posit that perceived depth is a monotonic function of  $\rho_i$ , which as we have shown is the optimal weighted sum of individual depth cues, scaled to unit variance. It follows immediately that IC has similarities to Fechnerian theories of sensory scaling, in that it predicts that perceived depth can be meaningfully measured in terms of just noticeable differences (JNDs).

To see why, suppose we have a disparity-defined stimulus  $d_A$  and a motion-defined stimulus  $v_A$ , both with a perceived depth of 10 cm, and also a disparity-defined stimulus  $d_B$  and a motion-defined stimulus  $v_B$  with a perceived depth of 11 cm.  $d_A$  and  $v_A$  have the same perceived depth, so according to IC they have the same value of  $\rho_i$ , which we can call  $\rho_A$ . Similarly,  $d_B$  and  $v_B$  both have  $\rho_i = \rho_B$ . Thus, the difference in the value of  $\rho_i$  between  $d_A$  and  $d_B$  is  $\rho_B - \rho_A$ , and the difference in  $\rho_i$  between  $v_A$  and  $v_B$  is also  $\rho_B - \rho_A$ . The variance of  $\rho_i$  is always one, so if depth JNDs are determined by the signal and the noise properties of  $\rho_i$  (as assumed by Domini et al., 2006), then the number of JNDs that separate  $d_A$  and  $d_B$  is the same as the number that separate  $v_A$  and  $v_B$ . For instance, if we define one JND as a separation of  $k$  standard deviations in the decision variable  $\rho_i$ , then  $d_A$  and  $d_B$  are separated by  $(\rho_B - \rho_A) / k$  JNDs, and so are  $v_A$  and  $v_B$ . Thus, IC predicts that any two depth-matched pairs of stimuli are separated by the same number of depth JNDs. (Note that even without our demonstration that PCP calculates an optimal weighted sum, Domini et al.'s Equation 7, which shows that  $\rho_i$  is proportional to true depth and has unit variance, implies this same conclusion.)

In classical Fechnerian theories, JNDs correspond to equal increments in subjective stimulus magnitude. In IC, JNDs correspond to equal increments in  $\rho_i$ , but perceived depth is an unknown monotonic function of  $\rho_i$ , so JNDs need not correspond to equal increments in perceived depth. Thus, IC is more akin to revisions of Fechner's theory that retain the JND as a unit of measurement but that allow the subjective perceptual increments corresponding to JNDs to vary as a function of baseline perceptual magnitude, e.g., an auditory JND may increase loudness more for loud sounds than for faint sounds (for a discussion of these and related issues, see Krueger, 1989).

In the following experiment, we examine the relationship between perceived depth and depth JNDs in order to test IC's prediction that they are tightly linked. We construct 3D stimuli with disparity as a depth cue and other 3D stimuli with motion as a depth cue. We match the perceived depth of each disparity stimulus to a motion stimulus. We measure the number of depth JNDs separating pairs of motion stimuli and also the number of depth JNDs separating the corresponding depth-matched pairs of

disparity stimuli. If IC is correct, then the number of JNDs separating pairs of motion-defined stimuli and pairs of depth-matched disparity-defined stimuli should be the same.

## Method

### Observers

Four observers participated in the experiment. Three were the authors, and the fourth was a York University undergraduate who was unaware of the purpose of the experiment. All observers reported having normal or corrected-to-normal vision.

### Stimuli

The stimuli were horizontally oriented random-dot half-cylinders (Figures 3 and 4), modelled closely on those of Domini et al. (2006). The stimuli measured 5.0 cm horizontally and vertically and subtended 2.9 degrees of visual angle at a viewing distance of 100 cm. Each half-cylinder was defined by 200 randomly placed dots, 3.6 arcmin in diameter. One axis of the elliptical cross-section of the cylinder was vertical in the frontoparallel plane and measured 5.0 cm. The other axis was along the line of sight, and its length varied from trial to trial. That is, the stimuli were horizontal half-cylinders, stretched or compressed along the observer's line of sight to varying degrees. A vertical depth gradient was created using either binocular disparity or motion. In the motion condition, a percept of depth was created by rocking the cylinder sinusoidally about a horizontal axis of rotation through the nearest point of the cylinder. The oscillation frequency was 1.0 Hz, and the amplitude was 10 degrees. All stimuli were shown for 1000 ms.

Stimuli were shown on a Dell UltraScan P991 19-in. CRT display with a 1024 × 768 resolution and a 120-Hz refresh rate. The display measured 34.5 × 26.0 cm and each pixel measured 0.35 mm. Stimuli were generated and displayed using MATLAB and the Psychophysics Toolbox (Brainard, 1997; Pelli, 1997) on an Apple G5 computer. All stimuli were viewed binocularly through Stereographics CrystalEyes LCD-shuttered glasses at a refresh rate of 60 Hz in each eye.

### Procedure

#### Depth matching

In the depth-matching part of the experiment, we matched the perceived depth of half-cylinders defined by disparity to half-cylinders defined by motion, individually for each observer. As reference stimuli, we used

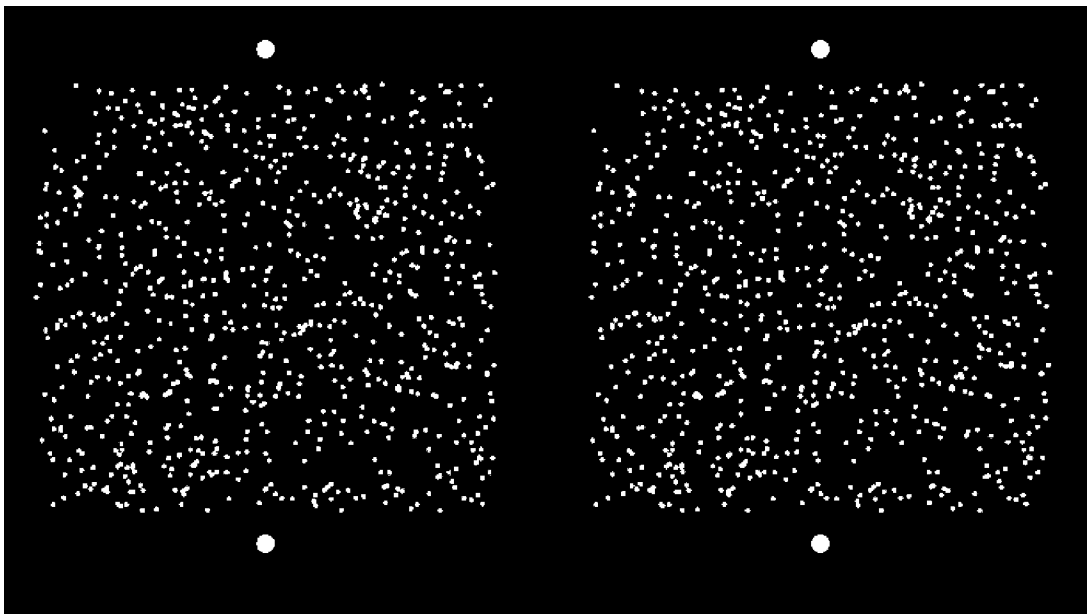


Figure 3. A typical disparity-defined stimulus from the experiment, showing a horizontally oriented half-cylinder. This figure is designed for cross-fusion, but in the experiment the stimuli were viewed through LCD-shuttered glasses and the large dots were not present.

motion-defined half-cylinders with simulated depths of 1.25 cm, 2.5 cm, and 5.0 cm. The vertical extent of the half-cylinders was 5.0 cm, so these stimuli were flatter than circular, circular, and deeper than circular, respectively. As test stimuli, we used disparity-defined half-cylinders with a range of simulated depths. Observers completed three blocks of 270 two-interval forced-choice (2IFC) trials,

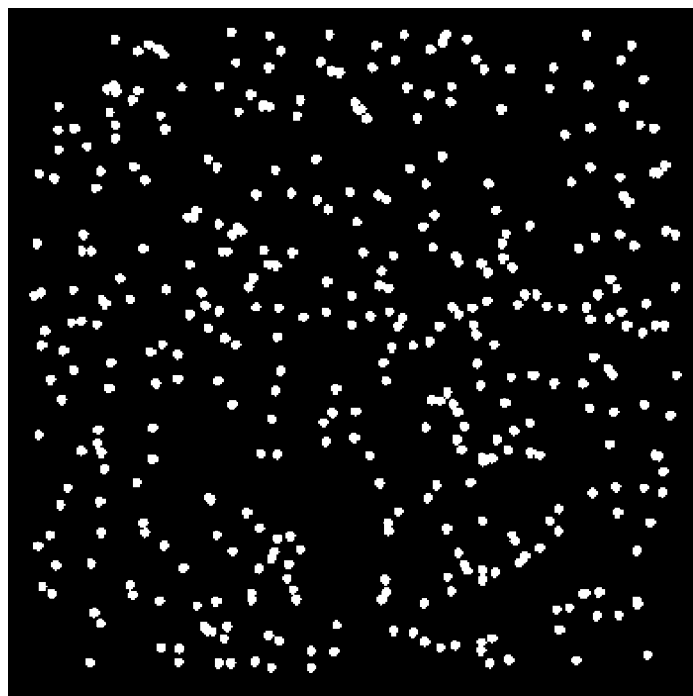


Figure 4. A typical motion-defined stimulus from the experiment, showing a horizontally oriented half-cylinder.

with only a single motion-defined reference depth shown in each block. On each trial, observers viewed a motion-defined reference stimulus and a disparity-defined test stimulus, in random order, separated by a blank interstimulus interval of 750 ms and pressed a key to indicate which interval contained the stimulus with the greater perceived depth. No feedback was given. The simulated depth of the test stimulus was chosen by the method of constant stimuli from a set of nine depths ranging from zero to twice the depth of the reference stimulus assigned to the block. All stimuli were viewed through LCD-shuttered stereo glasses, but the reference stimuli had zero disparity.

For each reference stimulus, we calculated the psychometric function indicating the probability of the observer choosing the disparity-defined test stimulus as having the greater perceived depth as a function of the simulated depth of the test stimulus. We fitted a Weibull cumulative distribution function to each psychometric function, and we took the fitted 50% probability point as the point of subjective equality, i.e., the simulated depth at which the disparity-defined test stimulus had the same perceived depth as the motion-defined reference stimulus.

### Depth discrimination

In the discrimination part of the experiment, we measured JNDs for the three motion-defined reference stimuli and the three depth-matched disparity-defined stimuli determined in the first part of the experiment. We call these the six *matched* stimuli. We measured the six JNDs in separate 270-trial blocks, i.e., only a single matched stimulus was shown in a given block. On each 2IFC trial, observers viewed a matched stimulus and a test

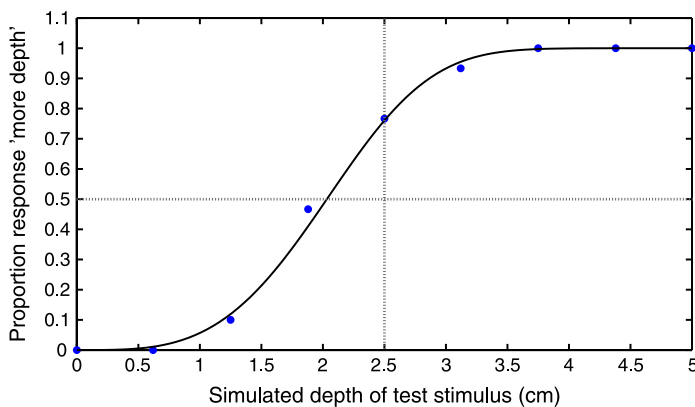


Figure 5. A psychometric function for a typical observer in the depth-matching condition. The reference stimulus was a motion-defined half-cylinder with a simulated depth of 2.5 cm (vertical dotted line). The x-axis indicates the simulated depth of the disparity-defined test stimulus, and the y-axis shows the proportion of times the observer chose the test stimulus as having the greater perceived depth.

stimulus, with the simulated depth of the test stimulus chosen by the method of constant stimuli. Disparity-defined matched stimuli were shown with disparity-defined test stimuli, and motion-defined matched stimuli were shown with motion-defined test stimuli. The stimuli were shown for 1000 ms, in random order, separated by a blank 750-ms interstimulus interval, and the observer pressed a key to indicate which interval contained the stimulus with the greater perceived depth. No feedback was given.

We defined a JND as the difference between the depths at which observers achieved 50% and 75% correct performance.

## Results and discussion

### Depth matching

Figure 5 shows a depth matching psychometric function for a typical observer. As expected, the probability of the observer reporting that the disparity-defined test stimulus had a greater perceived depth than the motion-defined reference stimulus increased smoothly as a function of the simulated depth of the test stimulus.

Figure 6 shows depth matches for all observers and indicates that there was an approximately linear relationship between the simulated depth of disparity-defined and motion-defined stimuli at the point of subjective equality. Furthermore, the disparity-defined stimuli had less simulated depth than the motion-defined stimuli at points of subjective equality, meaning that at a given simulated depth, motion-defined stimuli were perceived as being shallower than disparity-defined stimuli. This may be because the motion-defined stimuli had zero disparity, which was a cue that the stimuli were actually flat. In any case, this is not a problem for our test of IC: All we need

are two physically different sets of stimuli with matched perceived depths, and this is what the depth-matching part of the experiment provided.

### Depth discrimination

Figure 7 shows depth JNDs for all observers. JNDs increased approximately linearly as a function of stimulus depth, meaning that depth discrimination performance roughly followed Weber's law over the stimulus range tested (as found by McKee, Levi, & Bowne, 1990, for disparity-defined stimuli). This finding is itself important for our test of IC. According to IC, discrimination performance is based on the random variable  $\rho$ , which is proportional to true depth and has a variance that is independent of  $z$ . Thus, IC assumes that JNDs are the same at all depths, but this is clearly not the case.<sup>3</sup>

If JNDs were the same at all depths, we could count the number of JNDs separating two disparity-defined stimuli simply by dividing their simulated depth difference by the unique JND for disparity, and we could make the corresponding calculation for motion-defined stimuli. Now, though, we find that there is a different JND for each stimulus, so the simple calculation suggested by IC is not an appropriate way of counting JNDs.

Nevertheless, to remain true to the original formulation of IC, we performed this analysis. Figure 8 shows the number of JNDs separating disparity-defined and motion-defined pairs of stimuli, estimated using the JND from the shallower stimulus in each pair, and Figure 9 shows the same calculation but using the JND from the deeper stimulus in each pair. These figures indicate that depth-matched

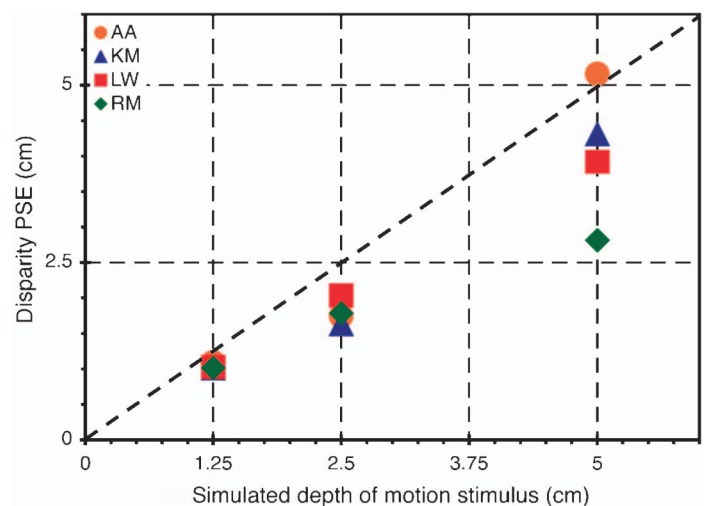


Figure 6. Depth matches for all observers. The x-axis indicates the simulated depth of the motion-defined reference stimulus, and the y-axis shows the simulated depth of the disparity-defined test stimuli at the point of subjective equality. The dotted diagonal line shows where depth matches would fall if motion-defined and disparity-defined stimuli with equal simulated depths also had equal perceived depths.

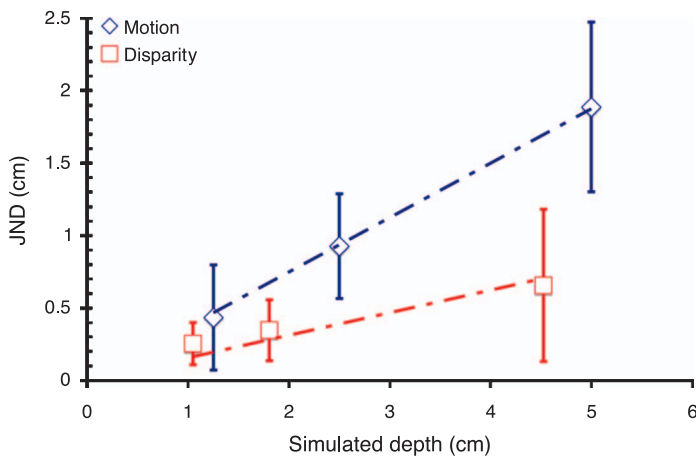


Figure 7. JND size as a function of baseline simulated depth, averaged over all four observers. The error bars indicate 95% confidence intervals. The dotted lines are maximum-likelihood fits of straight lines that pass through the origin. The slope of the disparity line is 0.13, and the slope of the motion line is 0.37.  $R^2$  is 0.91 for disparity and 0.99 for motion.

pairs of stimuli were not always separated by equal numbers of JNDs, contradicting IC’s prediction. However, these results should be regarded with caution because depth discrimination performance approximately followed Weber’s

law, so the calculation suggested by IC is not a valid way of counting the number of JNDs separating two stimuli.

The claim that perceived depth is measured out in JNDs is an interesting one, however, so to test this possibility we recalculated the number of JNDs separating the pairs of depth-matched stimuli in our experiment, this time taking into account Weber’s law. If the depth JND for a disparity-defined stimulus is proportional to the baseline stimulus depth,  $JND_D(z) = k_D z$ , then the number of JNDs separating disparity-defined stimuli at depths  $z_1$  and  $z_2$  is

$$n_D = \int_{z_1}^{z_2} (1/JND_D(z)) dz = \int_{z_1}^{z_2} (1/k_D z) dz \tag{6}$$

$$= (1/k_D)(\ln|z_2| - \ln|z_1|),$$

where  $\ln$  is the natural logarithm. Similarly, the number of JNDs separating motion-defined stimuli at depths  $z_1$  and  $z_2$  is

$$n_M = (1/k_M)(\ln|z_2| - \ln|z_1|), \tag{7}$$

where  $k_M$  is the constant of proportionality in Weber’s law for motion-defined stimuli,  $JND_M(z) = k_M z$ .

Figure 10 shows the number of JNDs separating pairs of motion-defined and disparity-defined stimuli, calculated

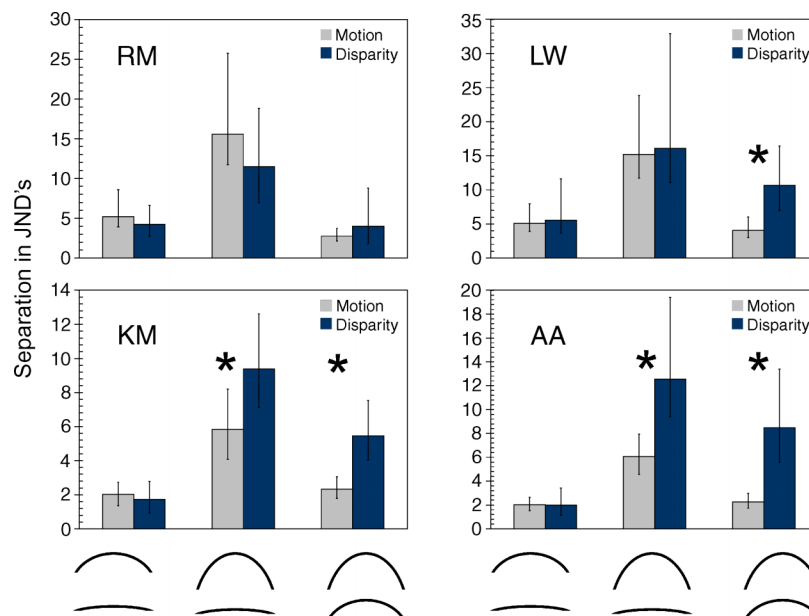


Figure 8. The number of JNDs separating each pair of motion-defined and disparity-defined stimuli, calculated using the JND from the shallower of each stimulus pair. In each panel, the leftmost bar shows the number of JNDs separating the 1.25-cm and the 2.5-cm motion-defined stimuli, and the immediately adjacent bar shows the number of JNDs separating the disparity-defined stimuli that were depth-matched to those two motion stimuli. The next pair of bars shows the number of JNDs between the 1.25-cm and the 5.0-cm motion stimuli and the corresponding depth-matched disparity stimuli. The third pair of bars shows the number of JNDs between the 2.5-cm and the 5.0-cm motion stimuli and the corresponding depth-matched disparity stimuli. The error bars indicate 95% confidence intervals, and asterisks indicate significantly different motion and disparity JND counts ( $p < 0.05$ , based on two-tailed bootstrap tests). Note that these JND counts are calculated using the formula derived from IC, which mistakenly assumes that JND size is independent of baseline stimulus depth. Hence, these JND counts are suspect.

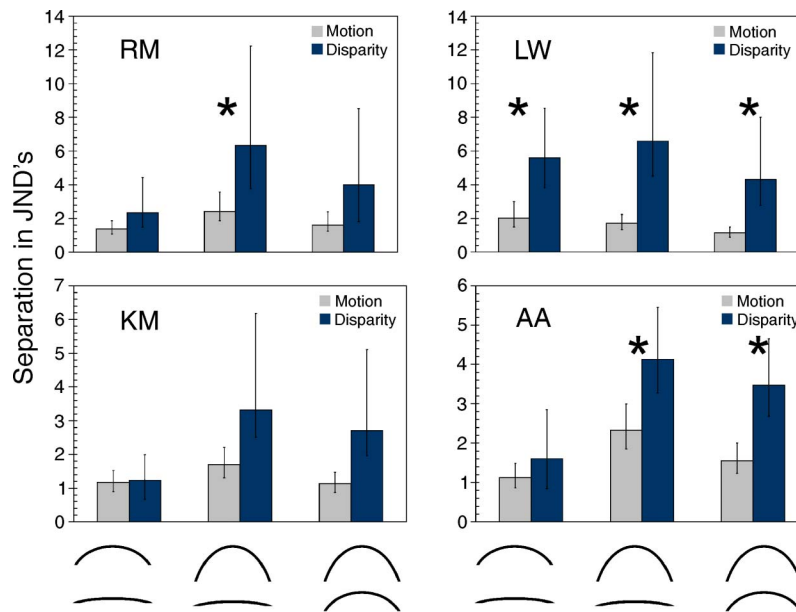


Figure 9. The number of JNDs separating each pair of motion-defined and disparity-defined stimuli, calculated using the JND from the deeper of each stimulus pair. See caption to Figure 8 for further information.

using Equations 6 and 7. We calculated the constants  $k_D$  and  $k_M$  individually for each observer by making a maximum-likelihood linear fit to JND size versus simulated depth (as in Figure 7, but using each observer’s JNDs instead of the group means). Even this revised calculation, which takes into account Weber’s law and thus gives a more accurate JND count, indicates that depth-matched motion and disparity stimuli were not separated by the same number of JNDs. In every comparison, the JND count was less for motion-defined

stimuli than for the corresponding disparity-defined stimuli. Not all of the JND counts shown in Figure 7 are independent, as the three motion JND counts are calculated from all three possible pairings of the three motion stimuli and similarly for the disparity JND counts. Nevertheless, even if we just consider the 1.25-cm vs. the 2.5-cm pairs and the 2.5-cm vs. the 5.0-cm pairs, this means that in eight cases the motion JND count was less than the disparity JND count, which is a statistically significant difference under a sign test ( $p < 0.01$ ).

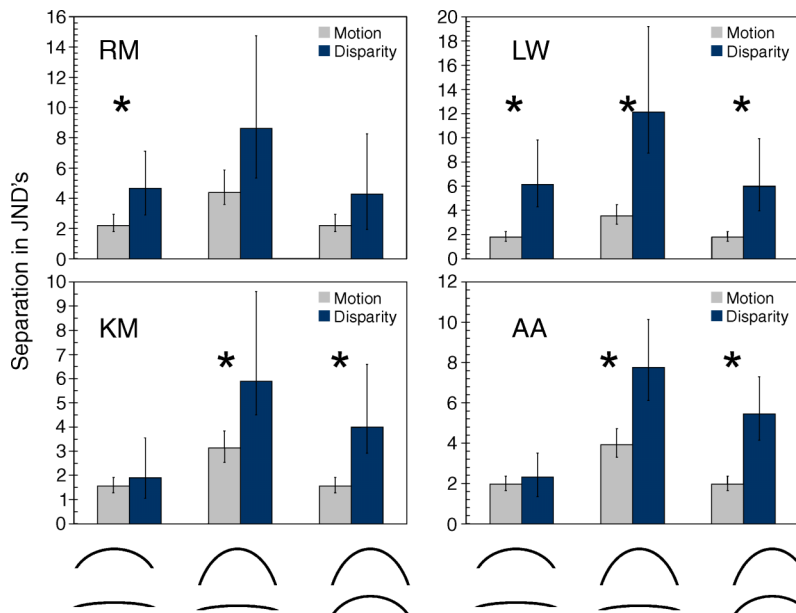


Figure 10. The number of JNDs separating each pair of motion-defined and disparity-defined stimuli, calculated using Equations 6 and 7. See caption to Figure 8 for further information.



Furthermore, several of the individual JND count comparisons were statistically significant as well ( $p < 0.05$ ). Thus, a key psychophysical prediction of IC is incorrect, even when we use a JND-counting formula that takes account of Weber's law.

## Conclusion

As far as we know, this experiment is the first test of a JND-counting model of perceived depth. Tests of the relationship between JND counts, sensory magnitudes, and stimulus intensity along other perceptual dimensions (e.g., brightness and loudness) have found that a simple sum of JNDs does not predict differences in sensory magnitudes (e.g., Newman, 1933; Stevens, 1961). Our results are consistent with this literature. However, given the number of proposed extensions and revisions of Fechner's account (see Krueger, 1989), a complete review of this issue is beyond the scope of this paper.

Domini et al. (2006) argue that their own empirical findings support IC and cannot be reconciled with MWF. We do not take issue with their conclusions, which address different aspects of IC than those we have discussed, e.g., they argue that IC correctly predicts that observers are largely unable to make metric depth estimates and only recover useful depth information up to an arbitrary affine transform. Many others have investigated similar claims (see Todd, 2004), and it is not our intent to review them here. Rather, our aim has been to investigate other implications of the IC model. In sum, we find that the separation between two objects as measured in JNDs does not predict their separation in perceived depth. This finding can be accommodated by theories like MWF that allow perceived depth and depth discriminability to vary independently, but it is problematic for theories like IC that imply that perceived depth and depth discriminability are closely linked.

## Appendix A

Given two Gaussian random variables,  $S \sim N(\mu_S, \sigma_S^2)$  and  $T \sim N(\mu_T, \sigma_T^2)$ , what weights maximize the SNR of the weighted sum  $C = \mu S + \nu T$ ?

The mean of the weighted sum is  $u\mu_S + \nu\mu_T$ , and the variance is  $u^2\sigma_S^2 + \nu^2\sigma_T^2$ , so the SNR is  $(u\mu_S + \nu\mu_T)/(u^2\sigma_S^2 + \nu^2\sigma_T^2)^{1/2}$ . Any two pairs of weights ( $u, \nu$ ) and  $(k_u, k_\nu)$  that differ only by a scale factor give the same SNR, so we will add the constraint that the variance of the weighted sum is one,  $u^2\sigma_S^2 + \nu^2\sigma_T^2 = 1$ . (The MWF model assumes  $u + \nu = 1$ , but the unit-variance constraint is more useful in our discussion of IC.)

We will use the method of Lagrange multipliers (Byron & Fuller, 1992). The objective function is the SNR,

$f(u, \nu) = (u\mu_S + \nu\mu_T)/(u^2\sigma_S^2 + \nu^2\sigma_T^2)^{1/2}$ , subject to the unit-variance constraint  $g(u, \nu) = u^2\sigma_S^2 + \nu^2\sigma_T^2 - 1 = 0$ . The Lagrangian is

$$\Lambda(u, \nu, \lambda) = f(u, \nu) + \lambda g(u, \nu), \quad (\text{A1})$$

$$= (u\mu_S + \nu\mu_T)/(u^2\sigma_S^2 + \nu^2\sigma_T^2)^{1/2} + \lambda(u^2\sigma_S^2 + \nu^2\sigma_T^2 - 1). \quad (\text{A2})$$

Setting  $\nabla \Lambda = 0$  and solving for  $u$  and  $\nu$ , we find

$$u = (\mu_S/\sigma_S^2)/\left((\mu_S/\sigma_S)^2 + (\mu_T/\sigma_T)^2\right)^{1/2}, \quad (\text{A3})$$

$$\nu = (\mu_T/\sigma_T^2)/\left((\mu_S/\sigma_S)^2 + (\mu_T/\sigma_T)^2\right)^{1/2}. \quad (\text{A4})$$

Thus, the optimal unit-variance weighted sum is

$$C = \frac{(\mu_S/\sigma_S^2)S + (\mu_T/\sigma_T^2)T}{\left((\mu_S/\sigma_S)^2 + (\mu_T/\sigma_T)^2\right)^{1/2}}. \quad (\text{A5})$$

## Acknowledgments

We thank Fulvio Domini and Michael Landy for helpful discussions. This research was funded by grants from the Natural Sciences and Engineering Research Council to RFM and LMW.

Commercial relationships: none.

Corresponding author: Kevin J. MacKenzie.

Email: k.j.mackenzie@bangor.ac.uk.

Address: School of Psychology, Adeilad Brigantia, Bangor University, Bangor, Gwynedd, LL57 2AS, UK.

## Footnotes

<sup>1</sup>This proportionality could be broken by creating cue conflict stimuli where disparity and motion specify different affine structures, and the analysis that follows does not apply in such unusual cases. Most cue conflict stimuli used to date, however, have specified the same affine depth structure in all cues, and have just assigned different depth scale factors to different cues.

<sup>2</sup>In this case, the principal component in Figure 2 will be vertical, and so the dot product  $\rho_i = (\bar{d}_i, \bar{v}_i) \cdot \bar{e}_1$  will be independent of  $\bar{d}_i$ .

<sup>3</sup>In order to accommodate Weber's law, IC would have to be revised to change the signal and noise properties of

the decision variable. Domini and Caudek (2007) have started investigations along these lines. However, incorporating Weber's law simply by making each cue's standard deviation proportional to the value of the cue will not work because then all normalized disparity measurements  $\bar{d}_i$  have the same expected value, as do all normalized velocity measurements  $\bar{v}_i$ , and the decision variable  $\rho$  is independent of true depth.

## References

- Brainard, D. H. (1997). The Psychophysics Toolbox. *Spatial Vision*, *10*, 433–436. [PubMed]
- Byron, F. W., & Fuller, R. W. (1992). *Mathematics of classical and quantum physics*. New York: Dover Publications, Inc.
- Domini, F., & Caudek, C. (2007, August 27–31). *A novel approach to the problem of cue integration*. European Conference on Visual Perception, Arezzo, Italy.
- Domini, F., Caudek, C., & Tassinari, H. (2006). Stereo and motion information are not independently processed by the visual system. *Vision Research*, *46*, 1707–1723. [PubMed]
- Ernst, M. O., & Banks, M. S. (2002). Humans integrate visual and haptic information in a statistically optimal fashion. *Nature*, *415*, 429–433. [PubMed]
- Hillis, J. M., Watt, S. J., Landy, M. S., & Banks, M. S. (2004). Slant from texture and disparity cues: Optimal cue combination. *Journal of Vision*, *4*(12):1, 967–992, <http://journalofvision.org/4/12/1/>, doi:10.1167/4.12.1. [PubMed] [Article]
- Jacobs, R. A. (1999). Optimal integration of texture and motion cues to depth. *Vision Research*, *39*, 3621–3629. [PubMed]
- Johnston, E. B., Cumming, B. G., & Landy, M. S. (1994). Integration of stereopsis and motion shape cues. *Vision Research*, *34*, 2259–2275. [PubMed]
- Krueger, L. E. (1989). Reconciling Fechner and Stevens: Toward a unified psychophysical law. *Behavioral and Brain Sciences*, *12*, 251–320.
- Landy, M. S., Maloney, L. T., Johnston, E. B., & Young, M. (1995). Measurement and modeling of depth cue combination: In defense of weak fusion. *Vision Research*, *35*, 389–412. [PubMed]
- Maloney, L. T., & Landy, M. S. (1989). A statistical framework for robust fusion of depth information. In W. A. Pearlman (Ed.), *Visual communications and image processing: IV. Proceedings of the SPIE* (vol. 1199, pp. 1154–1163).
- McKee, S. P., Levi, D. M., & Bowne, S. F. (1990). The imprecision of stereopsis. *Vision Research*, *30*, 1763–1779. [PubMed]
- Newman, E. B. (1933). The validity of the just noticeable difference as a unit of psychological magnitude. *Transactions of the Kansas Academy of Science*, *36*, 172–175.
- Oruç, I., Maloney, L. T., & Landy, M. S. (2003). Weighted linear cue combination with possibly correlated error. *Vision Research*, *43*, 2451–2468. [PubMed]
- Pelli, D. G. (1997). The VideoToolbox software for visual psychophysics: Transforming numbers into movies. *Spatial Vision*, *10*, 437–442. [PubMed]
- Stevens, S. S. (1961). To Honor Fechner and Repeal His Law: A power function, not a log function, describes the operating characteristic of a sensory system. *Science*, *133*, 80–86. [PubMed]
- Todd, J. T. (2004). The visual perception of 3D shape. *Trends in Cognitive Sciences*, *8*, 115–121. [PubMed]
- Young, M. J., Landy, M. S., & Maloney, L. T. (1993). A perturbation analysis of depth perception from combinations of texture and motion cues. *Vision Research*, *33*, 2685–2696. [PubMed]